

New NASICON type oxyanion high capacity anode, $\text{Li}_2\text{Co}_2(\text{MoO}_4)_3$, for lithium-ion batteries: preliminary studies

M. S. Michael · K. M. Begam · Michael Cloke ·
S. R. S. Prabaharan

Received: 24 July 2007 / Revised: 12 October 2007 / Accepted: 20 October 2007 / Published online: 21 November 2007
© Springer-Verlag 2007

Abstract We describe in this paper the lithium insertion/extraction behavior of a new NASICON type $\text{Li}_2\text{Co}_2(\text{MoO}_4)_3$ at a low potential and explored the possibility of considering this new oxyanion material as anode for lithium-ion batteries for the first time. $\text{Li}_2\text{Co}_2(\text{MoO}_4)_3$ was synthesized by a soft-combustion glycine-nitrate low temperature protocol. Test cells were assembled using composite $\text{Li}_2\text{Co}_2(\text{MoO}_4)_3$ as the negative electrode material and a thin lithium foil as the positive electrode material separated by a microporous polypropylene (Celgard® membrane) soaked in aprotic organic electrolyte (1 M LiPF_6 in EC/DMC). Electrochemical discharge down to 0.001 V from OCV (~3.5 V) revealed that about 35 Li^+ could possibly be inserted into $\text{Li}_2\text{Co}_2(\text{MoO}_4)_3$ during the first discharge (reduction) corresponding to a specific capacity amounting to 1,500 mAh g^{-1} . This is roughly fourfold higher compared to that of frequently used graphite electrodes. However, about 24 Li^+ could be extracted during the first charge. It is interesting to note that the same amount of Li^+ could be

inserted during the second Li^+ insertion process (second cycle discharge) giving rise to a second discharge capacity of 1,070 mAh g^{-1} . It was also observed that a major portion of lithium intake occurs below 1.0 V vs Li/Li^+ , which is typical of anodes being used in lithium-ion batteries.

Keywords Anode materials · Lithium cobalt molybdate · Lithium-ion battery · NASICON structure

Introduction

Lithium-ion cells have emerged as the technology of choice to the world of portable electronics. The total sale of the cells is enjoying an increasing pace every year. Lithium-ion cells available in the market make use of LiCoO_2 [1] as conventional positive electrodes, and the materials for negative electrodes are generally carbonaceous composites [2] so as to maintain a high-voltage character. Carbonaceous materials give a low voltage for lithium insertion/extraction and a long cycle life. However, the capacity of these materials is 370 mAh g^{-1} , which is considerably smaller than the capacity offered by lithium metal [3]. With the objective of overcoming these problems and for improving the performance of lithium-ion batteries, plenteous materials have been studied as possible candidates as anode [4–8].

Innovative methods were implemented to identify the anodic behavior of a few lithiated transition metal oxides besides their well known cathodic performance [9, 10] though not impressive in terms of cathode point of view. Notably, inverse spinel LiNiVO_4 being regarded as a signature of high voltage class cathode material exhibiting a high working voltage ≥ 4.8 V vs Li/Li^+ offers inferior specific capacity as cathode in lithium batteries [9]. Nevertheless, it was found to show a good anodic behavior

Contribution to ICMAT 2007, Symposium K: Nanostructured and bulk materials for electrochemical power sources, July 1-6, 2007, Singapore.

M. S. Michael
Department of Chemistry,
SSN College of Engineering,
SSN Nagar, Kalavakkam,
Chennai, India

K. M. Begam
Department of Electrical and Electronic Engineering,
Universiti Teknologi PETRONAS, Tronoh, Malaysia

M. Cloke · S. R. S. Prabaharan (✉)
Faculty of Engineering,
The Nottingham University, Malaysia Campus,
Semenyih, Malaysia
e-mail: Prabaharan.Sahaya@nottingham.edu.my

vs Li/Li^+ as negative electrode due to different oxidation states of the transition elements (V and Ni), which help in inserting Li^+ at very low discharge voltages [11–14]. Likewise, an analogous counterpart, LiCoVO_4 , for which the electrochemical properties as positive electrode were investigated earlier also demonstrated a high-energy density as novel anode [6]. Recently, it was reported that brannerite-type LiVMoO_6 show anodic characteristics in lithium rechargeable cells [15].

Our recent studies on oxyanion $\text{Li}_2\text{M}_2(\text{MoO}_4)_3$ [$\text{M}=\text{Ni}$, Co] materials as positive electrode (cathode) for lithium-containing cells suggest that cyclability (repeated charge/discharge) of these materials were hindered by drastic structural changes accompanied by exponential capacity decay [16–19]. Although these materials possess an open framework NASICON type structure, they did not demonstrate any useful electrochemical properties as cathodes for lithium batteries. Inspired by several recent reports on mixed transition metal oxides being investigated as negative electrodes [11–15] besides their positive electrode characteristics, we examined the anodic properties of $\text{Li}_2\text{Co}_2(\text{MoO}_4)_3$ in a lithium-containing cell in this paper. Interest in molybdenum-based oxide as anode material stems from its multivalent oxidation states. In this paper, we present the preliminary electrochemical results obtained on $\text{Li}_2\text{Co}_2(\text{MoO}_4)_3$ as anode in lithium batteries and describe the lithium insertion/extraction behavior at low potential.

Experimental

$\text{Li}_2\text{Co}_2(\text{MoO}_4)_3$ was synthesized by a soft-combustion approach as described elsewhere [16, 17] and annealed further at 500 and 600 °C to obtain a well-crystalline product. The phase purity and structure of the product was examined by employing a JEOL X-ray diffractometer, and scanning electron microscopy analysis was carried out to

obtain the grain size and morphology characteristics of the synthesized powders by using Cambridge Instruments as mentioned previously [17].

The anodic behavior of $\text{Li}_2\text{Co}_2(\text{MoO}_4)_3$ was observed by means of galvanostatic discharge/charge test performed on an automated battery-testing system (Arbin instruments BT2000, USA) equipped with MITSURO software. Negative electrodes were prepared from $\text{Li}_2\text{Co}_2(\text{MoO}_4)_3$ powders mixed with acetylene black and PTFE binder in the ratio 80:15:5 (weight), respectively. A thin lithium foil was used as the positive electrode, and the two electrodes were separated by a microporous polypropylene thin Celgard® membrane in a Teflon-based test cell. The electrolyte was 1 M LiPF_6 in EC/DMC (50:50 v/v) organic solution. Test cells were fabricated inside a glove box filled with high purity (99.999%) argon.

Results and discussion

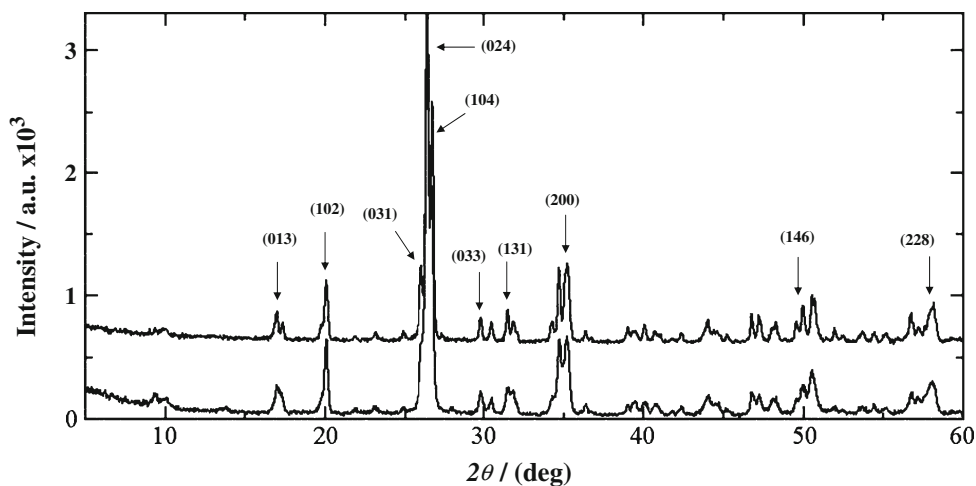
Phase analysis (XRD) and morphological analysis

Figure 1 shows the XRD pattern of $\text{Li}_2\text{Co}_2(\text{MoO}_4)_3$ [17]. It is clearly seen from Fig. 1 that increased annealing temperature results in better refinement of the diffraction peaks indicating the formation of a single phase product with high phase purity as explained in our previous publications [17]. The scanning electron micrograph for the $\text{Li}_2\text{Co}_2(\text{MoO}_4)_3$ powder annealed at 600 °C is presented in Fig. 2, which shows the formation of loosely agglomerated rod-like particles having a diameter within the 5- to 10- μm submicrometer range.

Electrochemical studies

Lithium insertion into $\text{Li}_2\text{Co}_2(\text{MoO}_4)_3$ was investigated under galvanostatic cycling at a constant current density of

Fig. 1 XRD patterns of $\text{Li}_2\text{Co}_2(\text{MoO}_4)_3$ at 500 °C (a) and 600 °C (b) annealing temperatures



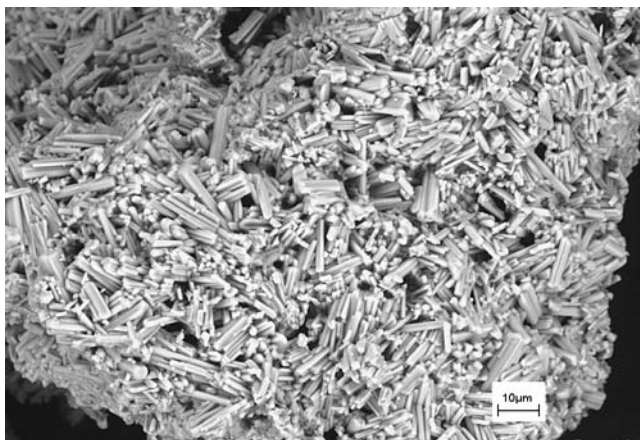
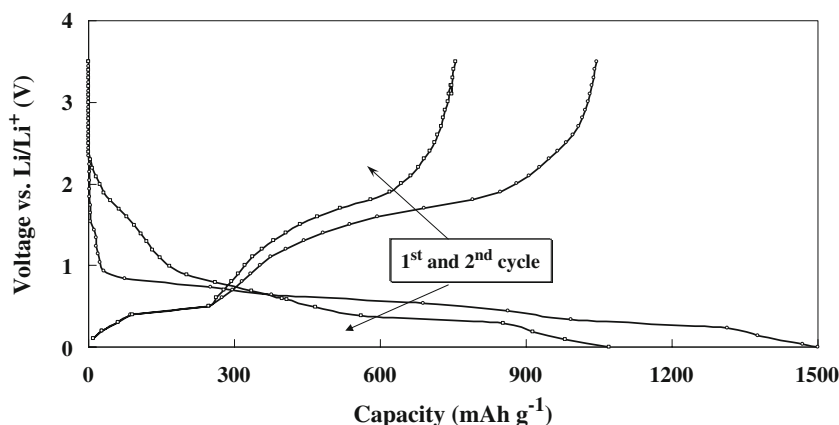


Fig. 2 SEM image of $\text{Li}_2\text{Co}_2(\text{MoO}_4)_3$ exhibiting submicron sized fiber-like rods

5 mA g^{-1} . Lithium insertion into the $\text{Li}_2\text{Co}_2(\text{MoO}_4)_3$ electrode begins with a discharge process while removal of lithium from the electrode is defined as a charge. Constant current (galvanostatic) discharge/charge curves of $\text{Li}/\text{Li}_2\text{Co}_2(\text{MoO}_4)_3$ test cell cycled between 3.5 and 0.001 V are depicted in Fig. 3 for the first two cycles.

It is apparent from the first discharge profile that there is no lithiation in $\text{Li}_2\text{Co}_2(\text{MoO}_4)_3$ up to 1.5 V right from OCV (3.5 V). The voltage drops vertically down to 1.5 V from where a plateau appears to proceed gradually, indicating an early stage of lithium intercalation process. The vertical fall from OCV up to 1.5 V vs Li/Li^+ is obviously attributed to the formation of thin passivation layer on to the electrode forming a solid electrolyte interface (SEI). The plateau appears to extend throughout the lithium reaction with the anode material, which may be considered as representing the ability of the material to accept large amounts of Li^+ in its framework structure. It was observed that the first lithiation corresponds to a discharge capacity of $1,500 \text{ mAh g}^{-1}$ with an insertion of approximately 35 Li^+ down to 0.001 V vs Li/Li^+ . This value is roughly fourfold higher compared to the capacity offered by graphitic anodes in lithium-ion batteries.

Fig. 3 First two discharge–charge curves of $\text{Li}_2\text{Co}_2(\text{MoO}_4)_3/\text{Li}$ test cell between 3.5 and 0.001 V. Current rate= 5 mA g^{-1} , weight of the active material= 0.04 g , electrolyte= 1 M LiPF_6 (EC/DMC). *Inset* showing the cell potential vs quantity of Li^+ insertion



However, upon first charge from 0.001 V, about 24 Li^+ could be removed from $\text{Li}_2\text{Co}_2(\text{MoO}_4)_3$, which is equivalent to 71% of the initial capacity. Kim et al. observed a similar irreversible capacity in the case of the MnV_2O_6 anode for which the first cycle charge capacity fade was estimated to be 57% (800 mAh g^{-1}) compared to its first discharge capacity ($1,400 \text{ mAh g}^{-1}$) [20]. Orsini et al. and Kim et al. also observed the same trend in LiNiVO_4 (inverse spinel) and crystalline MnMoO_4 , respectively, when these materials are used as anode [11, 21]. Hence, the studies on vanadates and molybdates suggest that the irreversible capacity fading arises from the electrolyte reduction leading to the formation of the SEI layer [5, 21–23]. Presumably, in the present case, the reduction of electrolyte at deep discharge potentials and hence the formation of the SEI layer could cause the irreversible capacity fade. However, this needs to be verified further using in situ/ex situ X-ray absorption studies (XAS).

It is fascinating to note that the same quantity of lithium-ions could be inserted during the subsequent discharge resulting in a second discharge capacity of $1,070 \text{ mAh g}^{-1}$. In addition, an interesting feature to be specified here is that the large capacity observed below approximately 1 V similar to $\text{LiTi}_2(\text{PO}_4)_3$ compounds having similar NASICON structure for which the discharge and charge capacity was mainly within 0.1–0.8 V vs Li/Li^+ [7]. This is a typical behavior of anodes of lithium-ion batteries.

The reaction of 35 Li^+ with $\text{Li}_2\text{Co}_2(\text{MoO}_4)_3$ is noteworthy and an appropriate mechanism is required to account for the excellent discharge capacity offered by the material. The possible changes in the oxidation states of metal cations during Li^+ insertion/removal in mixed transition metal oxycompounds containing MoO_4 polyhedra were investigated earlier. It was demonstrated by Wakihara et al. that Li insertion/removal in crystalline MnMoO_4 is accompanied by the valence change of Mo in addition to the role of the anion (oxygen ions) for charge compensation. Based on XANES measurement, they reported that Mo is reduced from $6+$ to $1+$ or $2+$ states at full lithiation and oxidized to

4+ upon Li removal while Mn retained in its 2+ state [21]. The V K-edge and Mn K-edge XANES measurements in Brannerite type MnV_2O_6 revealed that the valence of Mn goes to zero and that of V being 2+ in the fully lithiated MnV_2O_6 , and V is reversibly redoxed from 2+ to 4+ state whereas Mn valence exhibits no change after the initial Li insertion [22]. Lithiation in inverse spinel LiCoVO_4 reduces Co to metallic state and the valence of V varies reversibly during first cycle reaction [6]. Based on XAS studies on the LiNiVO_4 anode, Rossignol et al. reported that both V and Ni are reduced upon first lithiation and that vanadium regains the original oxidation state and nickel does not recover the pristine oxidation state during charge [5, 14]. These results imply the fact that the counter cation exhibits redox characteristics during Li^+ insertion/removal whether the other cation displays these properties.

In the present case, cobalt exists in 2+ oxidation state and the molybdenum being at 6+. In accordance with Li^+ insertion/removal in mixed transition metal oxycompounds as mentioned above, the insertion of Li^+ in $\text{Li}_2\text{Co}_2(\text{MoO}_4)_3$ could possibly be due to the gradual reduction of Mo from 6+ to its lowest oxidation state of 1+. As of now, there is no spectroscopic data available to confirm the valence state of cobalt upon completion of the reduction kinetics at approximately 0.001 V vs Li/Li^+ whether it exists in the metallic state and/or never reduced at all. XAS measurements will certainly provide such information concerning the valence state of the transition metal cations by means of in situ measurement techniques. These studies have been planned and the results will be reported elsewhere in the near future. Upon extraction of Li^+ during oxidation (charge reaction), molybdenum goes to its higher oxidation states as evidenced from the first charge curve and the following discharge/charge profiles. Figure 3 clearly demonstrates the reversible nature of $\text{Li}_2\text{Co}_2(\text{MoO}_4)_3$ when cycled in lithium-containing cell as anode.

It is obviously understood that reduction of the cations alone may not account for such an unusual large capacity obtained in $\text{Li}_2\text{Co}_2(\text{MoO}_4)_3$. Plausible explanation being, as proposed recently, that oxygen acts as a redox center in Li–O bonds besides the possible valence change in transition metal cations during the insertion/extraction of lithium [12, 22]. We invoke similar thoughts to account for such a large capacity realized in the present material although this still awaits explicit experimental proof. The role of anions in the lithium insertion/removal process was suggested in anode materials such as nitrides [24] and vanadium oxide materials [25]. The N K-edge EELS study, whose spectra are essentially the same as XANES, on the anode material $\text{Li}_{2.6}\text{Co}_{0.4}\text{N}$ have showed that Li^+ extraction decreases the occupancy of the nitrogen 2p orbitals [26]. This indicates that nitrogen orbitals besides those of Co play an important

role in keeping the charge balance. Ceder and coworkers proposed that oxygen atoms function as electron acceptors upon insertion of Li^+ into metal-oxides and metal-dichalcogenides [27, 28]. It is interesting to note that this was clearly pointed out by Wakihara et al. that there is strong hybridization of the Mo 4d band with the O 2p band in MnMoO_4 and eventually the Mo–O bond has strong covalent character [21]. Accordingly, it is likely in the present case that Mo 4d orbital gets possibly mixed with O 2p orbital, which reduces oxygen besides molybdenum to accommodate the huge amount of Li^+ intake into the host structure leading to a very high capacity.

Nevertheless, it is felt necessary to investigate further to find out the precise mechanism for the electrochemical Li^+ insertion/removal in $\text{Li}_2\text{Co}_2(\text{MoO}_4)_3$ by using in situ XAS studies and to open avenues for further research. The work is underway to establish the Li^+ mechanism leading to large insertion of Li^+ and will be published elsewhere.

Conclusion

Soft-combustion-derived NASICON type $\text{Li}_2\text{Co}_2(\text{MoO}_4)_3$ was found to exhibit interesting electrochemical characteristics as anode in rechargeable lithium batteries. Preliminary studies prove that the reaction of lithium within the NASICON framework of $\text{Li}_2\text{Co}_2(\text{MoO}_4)_3$ is reversible by exhibiting a discharge capacity of approximately 1,500 mAh g^{-1} amounting to 35 Li^+ . Thus, the material was found to offer a high discharge capacity during the first lithium insertion process, approximately fourfold higher than the capacity offered by traditional graphitic anodes being used in commercial lithium-ion cells. Nevertheless, approximately 24 Li^+ could be extracted during the first charge (removal of lithium). It is interesting to note that the same amount of lithium-ions could be inserted during the second Li^+ insertion process (second cycle discharge) giving rise to a second discharge capacity of 1,070 mAh g^{-1} . It was also observed that a major portion of lithium intake occurs below 1 V, which is typical of a characteristic anode for lithium-ion batteries.

References

1. Mizushima K, Jones PC, Wiseman PJ, Goodenough JB (1980) Mater Res Bull 15:783
2. Sawai K, Iwakoshi Y, Ohzuku T (1994) Solid State Ion 69:273
3. Koch VR, Goldman JL, Mattos CJ, Mulvaney M (1982) J Electrochem Soc 264:22
4. Poizot P, Laruelle S, Grugeon S, Dupont L, Tarascon J-M (2001) J Power Sources 97–98:235

5. Rossignol C, Ouvrard G, Baudrin E (2001) *J Electrochem Soc* 148:A869
6. Shirakawa J, Nakayama M, Ikuta H, Uchimoto Y, Wakihara M (2004) *Electrochem Solid-state Lett* 7:A27
7. Wang GX, Bradhurst DH, Dou SX, Liu HK (2003) *J Power Sources* 124:231
8. Burba CM, Frech R (2005) *J Electrochem Soc* 152:A1233
9. Fey GTK, Li W, Dahn JR (1994) *J Electrochem Soc* 141:2279
10. Michael MS, Fauzi A, Prabaharan SRS (2000) *Int J Inorg Mater* 2:261
11. Orsini F, Baudrin E, Denis S, Dupont L, Touboul M, Guyomard D, Piffard Y, Tarascon J-M (1998) *Solid State Ion* 107:123
12. Denis S, Baudrin E, Touboul M, Tarascon JM (1997) *J Electrochem Soc* 144:4099
13. Denis S, Baudrin E, Orsini F, Ouvrard G, Touboul M, Tarascon JM (1999) *J Power Sources* 81–82:79
14. Rossignol C, Ouvrard G (2001) *J Power Sources* 97–98:491
15. Liang Y, Yang S, Yi Z, Li M, Sun J, Zhou Y (2005) *J Mater Sci Lett* 40:5553
16. Begam KM, Michael MS, Taufiq-Yap YH, Prabaharan SRS (2004) *Electrochem Solid-state Lett* 7:A242
17. Prabaharan SRS, Ramesh S, Michael MS, Begam KM (2004) *Mater Chem Phys* 87:318
18. Prabaharan SRS, Michael MS, Begam KM (2004) *Electrochem Solid-state Lett* 7:A416
19. Begam KM, Prabaharan SRS (2006) *J Power Sources* 159:319
20. Kim SS, Ikuta H, Wakihara M (2001) *Solid State Ion* 139:57
21. Kim SS, Ogura S, Ikuta H, Uchimoto Y, Wakihara M (2002) *Solid State Ion* 146:249
22. Hara D, Shirakawa J, Ikuta H, Uchimoto Y, Wakihara M, Miyanaga T, Watanabe I (2002) *J Mater Chem* 12:3717
23. Laruelle S, Poizot P, Baudrin E, Briosis V, Touboul M, Tarascon J-M (2001) *J Power Sources* 97–98:251
24. Shodai T, Sakurai Y, Suzuki T (1999) *Solid State Ion* 122:85
25. Denis S, Baudrin E, Touboul M, Tarascon JM (1997) *J Electrochem Soc* 144:3886
26. Suzuki S, Shodai T, Yamaki J (1998) *J Phys Chem Solids* 59:331
27. Aydinol MK, Kohan AF, Ceder G, Cho K, Joannopoulos J (1997) *Phys Rev B* 56:1354
28. Ceder G, Chiang YM, Sadoway DR, Aydinol MK, Jiang YI, Huang B (1998) *Nature* 392:694